

RECENT RESULTS ON JET PHYSICS AT THE TEVATRON

M. Martínez

ICREA/Institut de Física d'Altes Energies. Barcelona, 01893-E, Spain.

In this contribution, a comprehensive review of the main aspects of high p_T jet physics in Run II at the Tevatron is presented. Recent measurements on inclusive jet and dijet production are discussed using different jet algorithms and covering a wide region of jet transverse momentum and jet rapidity. Several measurements, sensitive to a proper description of soft gluon radiation and the underlying event in hadron collisions, are also shown.

1 Inclusive Jet Production

The measurement of the inclusive jet cross section in $p\bar{p}$ collisions at $\sqrt{s} = 1.96$ TeV constitutes a stringent test of perturbative QCD (pQCD) predictions over almost nine orders of magnitude. The increased center-of-mass energy and integrated luminosity in Run II at the Tevatron allows to search for signals of quark compositeness down to $\sim 10^{-19}$ m. Both CDF and D0 experiments have explored new jet algorithms away from the cone-based jet algorithm employed in Run I that was not infrared safe.

The CDF experiment has published results^{1,2} on inclusive jet production using both the k_T ^{3,4} and a midpoint⁵ algorithms. While the k_T algorithm is infrared safe to all orders in perturbation theory, the midpoint algorithm employed still suffers from some infrared sensitivity at higher orders. The measurements are performed for jets with $p_T^{\text{jet}} > 54$ GeV/c and rapidity in the region $|y^{\text{jet}}| < 2.1$, using 1.0 fb^{-1} of data. Figure 1(left) shows the measured cross sections

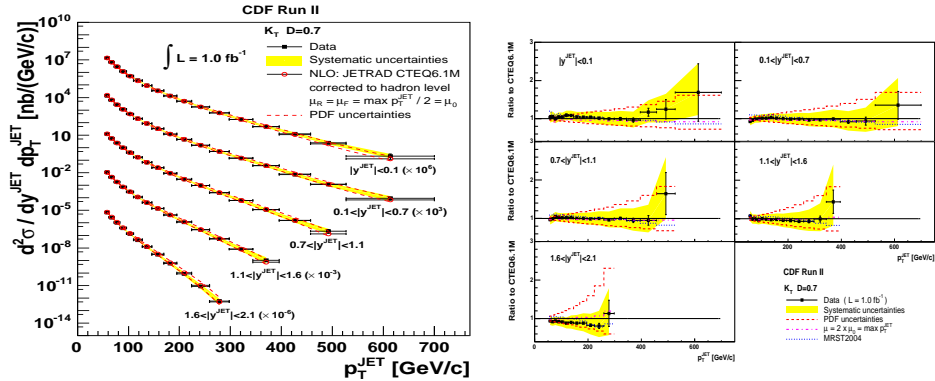


Figure 1: Measured inclusive differential jet cross sections, using the k_T algorithm with $D = 0.7$, as a function of p_T^{jet} in different $|y^{\text{jet}}|$ regions compared to NLO pQCD predictions. The shaded bands show the total systematic uncertainty on the measurements. The dashed lines indicate the PDF uncertainty on the theoretical predictions.

using the k_T algorithm, with $D = 0.7$, compared to NLO pQCD predictions⁶, which include

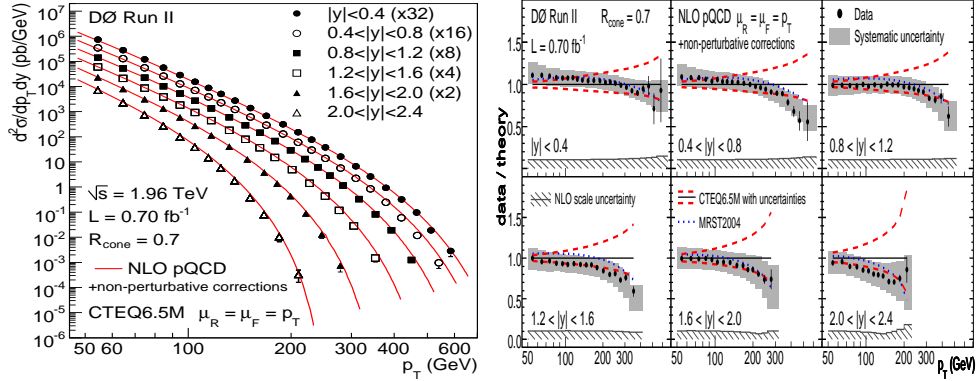


Figure 2: (left) Measured inclusive jet cross section as a function of p_T^{jet} in different $|y^{\text{jet}}|$ ranges compared to pQCD NLO predictions. (right) Ratio data/theory as a function of p_T^{jet} in different $|y^{\text{jet}}|$ ranges. The bands indicate the uncertainty on the data and the dashed lines the uncertainty on the NLO prediction using CTEQ6.5M PDFs. The dotted lines show the ratio to MRST2004 PDFs.

non-pQCD corrections relevant at low p_T^{jet} . The measured cross sections decrease by more than seven to eight orders of magnitude as p_T^{jet} increases. Figure 1(right) shows the ratios data/theory as a function of p_T^{jet} . Good agreement is observed in the whole range in p_T^{jet} and y^{jet} between the measured cross sections and the theoretical predictions. In the most forward region, the uncertainty on the measured cross section at high p_T^{jet} , compared to that on the theoretical prediction, already indicated that the data would contribute to a better understanding of the gluon PDF. In the region $0.1 < |y^{\text{jet}}| < 0.7$, different values for D in the k_T algorithm are considered: $D = 0.5$ and $D = 1.0$, thus decreasing and increasing the effective size of the jet and therefore the non-pQCD contributions, respectively. In both cases, good agreement is observed between the measured cross sections and the NLO pQCD predictions.

Similarly, Figure 2 shows the measured inclusive jet cross sections by D0⁷ based on 0.7 fb $^{-1}$ of Run II data. The midpoint jet algorithm has been used with a cone size $R=0.7$. The measurements are carried out for jets with $p_T^{\text{jet}} > 50$ GeV/c in six different rapidity regions up to $|y^{\text{jet}}| < 2.4$. The data are compared to NLO pQCD predictions, as implemented in the NLO++⁸ program, with CTEQ6.5M and MRST2004 PDFs sets, and using p_T^{jet} as the nominal renormalization/factorization scale. Figure 2(right) presents the ratio data vs NLO pQCD predictions as a function of p_T^{jet} in the different $|y^{\text{jet}}|$ regions. The measurements are in good agreement with the theoretical predictions within the current PDFs uncertainties. However, the Figure also suggests that the data prefer the lower edge of the CTEQ uncertainty band while the measurements are in good agreement with the nominal MRST2004 prediction.

The CDF and D0 experiments have employed the dijet invariant mass distribution to search for resonances decaying into jets⁹ as predicted by different models. In the case of D0, measurements of the dijet angular distributions are performed in different regions of the dijet invariant mass. For both experiments, good agreement is observed between the data and theory, and the results are translated into improved limits in different models. In particular, compositeness scales Λ below 2.56 TeV are now excluded at 95% C.L.

2 Jet Shapes

The internal structure of jets is dominated by multi-gluon emissions from the primary final-state parton. It is sensitive to the relative quark- and gluon-jet fraction and receives contributions from soft-gluon initial-state radiation and beam remnant-remnant interactions. The study of jet shapes at the Tevatron provides a stringent test of QCD predictions and tests the validity of the models for parton cascades and soft-gluon emissions in hadron-hadron collisions. The CDF

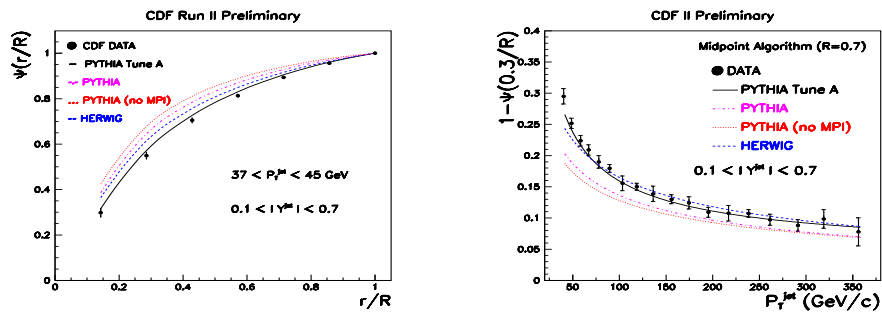


Figure 3: (left) The measured integrated jet shape, $\Psi(r/R)$, in inclusive jet production for jets with $0.1 < |y^{\text{jet}}| < 0.7$ and $37 \text{ GeV}/c < p_T^{\text{jet}} < 45 \text{ GeV}/c$. The predictions of PYTHIA-TUNE A (solid lines), PYTHIA (dashed-dotted lines), PYTHIA-(no MPI) (dotted lines) and HERWIG(dashed lines) are shown for comparison. (right) The measured $1 - \Psi(0.3/R)$ as a function of p_T^{jet} for jets with $0.1 < |y^{\text{jet}}| < 0.7$ and $37 \text{ GeV}/c < p_T^{\text{jet}} < 380 \text{ GeV}/c$.

experiment has published results¹⁰ on jet shapes for central jets with transverse momentum in the region $37 < p_T^{\text{jet}} < 380 \text{ GeV}$, where jets are searched for using the midpoint algorithm and a cone size $R = 0.7$. The integrated jet shape, $\Psi(r)$, is defined as the average fraction of the jet transverse momentum that lies inside a cone of radius r concentric to the jet cone:

$$\Psi(r) = \frac{1}{N_{\text{jet}}} \sum_{\text{jets}} \frac{P_T(0, r)}{P_T(0, R)}, \quad 0 \leq r \leq R \quad (1)$$

where N_{jet} denotes the number of jets. The measured jet shapes have been compared to the predictions from PYTHIA-TUNE A and HERWIG Monte Carlo programs. In addition, two different PYTHIA samples have been used with default parameters and with and without the contribution from multiple parton interactions (MPI) between proton and antiproton remnants, the latter denoted as PYTHIA-(no MPI), to illustrate the importance of a proper modeling of soft-gluon radiation in describing the measured jet shapes. Figure 3 presents the measured integrated jet shapes, $\Psi(r/R)$, for jets with $37 < p_T^{\text{jet}} < 45 \text{ GeV}$, compared to HERWIG, PYTHIA-TUNE A, PYTHIA and PYTHIA-(no MPI) predictions. Figure 3(right) shows, for a fixed radius $r_0 = 0.3$, the average fraction of the jet transverse momentum outside $r = r_0$, $1 - \Psi(r_0/R)$, as a function of p_T^{jet} . The measurements indicate that the jets become narrower as p_T^{jet} increases. PYTHIA with default parameters produces jets systematically narrower than the data in the whole region in p_T^{jet} while PYTHIA-TUNE A predictions describe all of the data well.

3 Dijet Azimuthal Decorrelations

The D0 experiment has employed the dijet sample to study azimuthal decorrelations, $\Delta\phi_{\text{dijet}}$, between the two leading jets¹¹. The normalized cross section,

$$\frac{1}{\sigma_{\text{dijet}}} \frac{d\sigma}{d\Delta\phi_{\text{dijet}}}, \quad (2)$$

is sensitive to the spectrum of the gluon radiation in the event. The measurements has been performed in different regions of the leading jet p_T^{jet} starting at $p_T^{\text{jet}} > 75 \text{ GeV}$, where the second jet is required to have at least $p_T^{\text{jet}} > 40 \text{ GeV}$. Figure 4 shows the measured cross section compared to LO and NLO pQCD predictions¹². The LO (non trivial) predictions for this observable, with at most three partons in the final state, is limited to $\Delta\phi_{\text{dijet}} > 2\pi/3$, for which the three partons define a *Mercedes-star* topology. The NLO predictions for this observable,

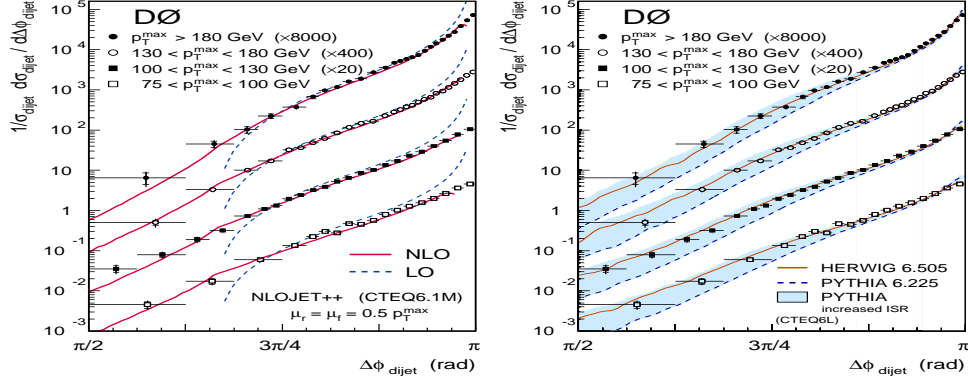


Figure 4: (left) Measured azimuthal decorrelations in dijet production for central jets compared to pQCD predictions in different regions of p_T^{jet} of the leading jet. (right) Measured azimuthal decorrelations in dijet production for central jets compared to PYTHIA and HERWIG predictions in different regions of leading p_T^{jet} . The band covers PYTHIA predictions with different amount of initial-state soft-gluon radiation.

with four partons in the final state, describes the measured $\Delta\phi_{\text{dijet}}$ distribution better except in the very high and very low regions of $\Delta\phi_{\text{dijet}}$. Figure 4(right) present the measured cross section compared to PYTHIA and HERWIG predictions in different regions of p_T^{jet} . The PYTHIA samples with default parameters underestimates the gluon radiation at large angles. Different tunes of PYTHIA predictions are possible, which include an enhanced contribution from initial-state soft gluon radiation, to properly describe the azimuthal distribution. HERWIG also describes the data although tends to produce less radiation than PYTHIA close to the direction of the leading jets. This measurement clearly shows that angular correlations between jets can be employed to tune Monte Carlo predictions of soft gluon radiation in the final state.

Acknowledgments

I would like to thank organizers for their kind invitation to the conference.

References

1. A. Abulencia *et al.* (CDF Collaboration), Phys. Rev. Lett. **96**, 122001 (2006).
A. Abulencia *et al.* (CDF Collaboration), Phys. Rev. D **75**, 092006 (2007).
2. A. Abulencia *et al.* (CDF Collaboration), Phys. Rev. D **74**, 071103(R) (2006).
T. Aaltonen *et al.* (CDF Collaboration), hep-ex/0807.2204
3. S. Catani *et al.*, Nucl. Phys. B **406**, 187 (1993).
4. S.D. Ellis and D.E. Soper, Phys. Rev. D **48**, 3160 (1993).
5. G. C. Blazey, et al., hep-ex/0005012 (2000).
S.D. Ellis, et al., hep-ph/0111434 (2001).
6. W.T. Giele, E.W.N. Glover and David A. Kosower, Nucl. Phys. B **403**, 633 (1993).
7. V. M. Abazov *et al.* (DØ Collaboration), Phys. Rev. Lett. **101**, 062001 (2008).
8. T. Kluge, K. Rabbertz, and M. Wobisch, arXiv:hep-ph/0609285.
Z. Nagy, Phys. Rev. D **68**, 094002 (2003).
9. D0 Collaboration, Note 5733-CONF. CDF Collaboration, hep-ex/0812.4036.
10. D. Acosta *et al.* (CDF Collaboration), Phys. Rev. D **71**, 112002 (2005).
11. V.M. Abazov *et al.* (DØ Collaboration), Phys. Rev. Lett. **94**, 221801 (2005).
12. Z. Nagy, Phys. Rev. Lett. **88**, 122003 (2002).